P. Garcia-Navarro<sup>2</sup>, M. E. Hubbard and A. Priestley Dept. of Mathematics, P.O. Box 220,

<sup>&</sup>lt;sup>1</sup>The first author was funded by the EC Program of Human Capital and Mobility, the second by DRA Farnborough and the third by the U.K. S.E.R.C.

<sup>&</sup>lt;sup>2</sup>on leave from the University of Zaragoza

## Abstract

A multidimensional upwinding technique is applied to the simulation of 2D shallow water flows. It is adapted from fluctuation splitting methods recently proposed for the solution of the uler system of equations on unstructured triangular grids. The basis of the numerical method is stated and the particular adaptation to the shallow water system is described. Numerical results of interest to hydraulic engineers are presented. Despite the complexities of the scheme advantages related to the use of a discretisation based on triangles would seem to make the schemes competitive with those currently in use.

## 1 Introduction

In reading the literature of recent years on the latest advances in numerical methods for hyperbolic conservation laws, one might gain the impression that many more people worked on problems involving the uler equations than on problems concerning the shallow water equations. In practice, though, this is not the situation, with many more engineers, physicists and mathematicians being involved in solving problems of the latter kind on a day to day basis.

Classical methods and central difference schemes still dominate the commercial software products for this market, with Preissmann's, Abbott's (see [4] for example) and McCormack's [7] schemes the most commonly used. These schemes are well known to require special treatment in many situations so that the calculations may proceed.

Some years after their adoption for solving problems in gas dynamics, upwind and TVD (Total Variation Diminishing) numerical schemes have been successfully used for the solution of the shallow water equations, with similar advantages [8]. Their use is nevertheless only gradually gaining acceptance in this sector.

Recently, in the context of gas dynamics, doubt has been expressed as to whether the essentially 1D TVD schemes are the most suitable choice for multi-dimensional calculations, and the search has been initiated for genuinely multi-dimensional approaches. Most of these are based on piecewise constant representations of the solution on triangular grids with a 1D upwinding of the Riemann problem for each edge of the triangle. However, it has been claimed that such an approach is weak when the solution is not constant along a triangle edge, since it may misinterpret features which are not aligned with grid interfaces.

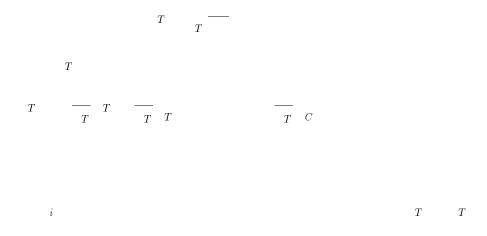
In a different philosophy, instead of concentrating on finite volumes and the changes of the variables across the cell sides, Deconinck et al. [5] consider solutions on triangular grids in which the unknowns are associated with the vertices and updates to these nodal values are through the advection of linear wave solutions. This avoids the problems of taking the normal to the cell interfaces as a privileged direction.

Reference [5] is concerned with gas dynamics applications. In this paper we consider the use of this technique for 2D shallow water flows and the question of whether they may be of practical use. In the next sections, the basis of the numerical method is stated and the adaptation to the shallow water system is described. The numerical treatment of the boundaries as well as the inclusion of source terms in the governing equations are also discussed. Finally, some numerical results are presented. Although this work is at an early stage, our results indicate that the advantages may outweigh the disadvantages and that these schemes may have a future for hydraulic engineering applications.

For the numerical solution of the 2D linear scalar equation

$$--+ = 0 = \begin{pmatrix} x & y \end{pmatrix} \tag{2.1}$$

with constant , we assume the given physical domain to be discretised by triangular cells and a set of initial values  $_i$  stored at the nodes of the mesh. For each cell T, of area  $_T$ , a cell fluctuation is defined as



 $T \qquad \frac{3}{T} \qquad i \qquad i$   $T \qquad T \qquad T$  3  $T \qquad i \qquad i$  i=1

i – i

the technique.

Residuals and fluctuations are cell-based quantities which are going to be used for the updating of the nodal values. For this purpose we introduce distribution coefficients,  $i_T$ , defining the weightings of the residual to the nodes in a cell. For conservation and consistency they must satisfy

$$\int_{i=1}^{3} T = 1$$

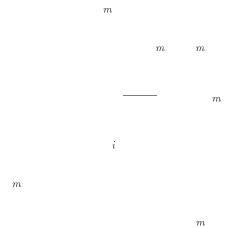
in every cell, see [5] for example. Then, a first order explicit time-stepping procedure at the nodes can be defined as

$$i^{n+1} = i \quad \frac{\Delta}{i} \quad T \quad T \quad T$$
 (2.8)

where the sum is over all the cells meeting at node , and where  $_{i}=\frac{1}{3}$   $_{T_{i}}$   $_{T}.$ In order to focus on the individual cell treatment, the advection scheme can be expressed, on each triangle, as

where only the influence from the individual triangle has been included.

There exist many criteria for the design of advection schemes, depending on the choice of the distribution coefficients. Two properties are of interest, positivity and linearity preservation of the scheme. The former is related to the 1D property of monotonicity whilst the second has to do with the accuracy of the method. Unfortunately, their simultaneous requirement is incompatible with



If the equation to be solved is non-linear, a suitable linearization must be performed before the techniques described for the linear equation are applied. Given the non-linear equation

$$---+$$
 ( ) = 0 = ( )

where

the fluctuation is defined as

$$\Phi_T = {}_T$$

x y

Where, in particular, a consistent approximation for the cell residual is sought

$$_{T} = (\bar{A}, \bar{B})_{T} \qquad _{T} \tag{2.10}$$

where  $\bar{A}_T$ ,  $\bar{B}_T$  are discrete equivalents of the cell averaged Jacobian matrices, calculated using the nodal values. The assumption of linear variation of — on each cell, enables us to write

$$T = \frac{1}{S_T} {}_T(A,) \qquad dS$$
$$= \frac{1}{S_T} {}_T(A,B)dS \qquad (2.11)$$

where discrete cell gradients and cell Jacobians can be defined in the same form as for the scalar case

$$T = \frac{1}{S_T} \int_{i=1}^{3} i \, i \, i$$

$$\bar{A} = \frac{1}{S_T} \int_{T} A dS$$

$$\bar{B} = \frac{1}{S_T} \int_{T} B dS$$

Unfortunately, the exact evaluation of the above integrals is not practical either for the uler or for the shallow water equations. Roe [13] suggested the introduction of a parameter set of variables for a simpler treatment of the former system. The strategy we have followed for the shallow water equations makes use of the set of primitive variables and is described in the next section.

We begin this section by writing the homogeneous version of the system of equations in terms of the conserved variables,

$$= (h, uh, vh)^{T}, (3.1)$$

where and are the depth and velocities respectively, that is,

$$---+---=0$$
 (32)

where the fluxes are,

$$\mathbf{E} = \begin{pmatrix} uh \\ u^2h + \frac{gh^2}{2} \\ uvh \end{pmatrix} , \quad \mathbf{F} = \begin{pmatrix} vh \\ uvh \\ v^2h + \frac{gh^2}{2} \end{pmatrix}.$$

It can be rewritten in terms of the same variables but in a non-conservative form as,

$$\frac{\partial \mathbf{U}}{\partial t} + A \frac{\partial \mathbf{U}}{\partial x} + B \frac{\partial \mathbf{U}}{\partial y} = 0 \tag{3.3}$$

in which the two Jacobian matrices are

$$A = \frac{\partial \mathbf{E}}{\partial \mathbf{U}} = \begin{pmatrix} 0 & 1 & 0 \\ -u^2 + gh & 2u & 0 \\ -uv & v & u \end{pmatrix} , B = \frac{\partial \mathbf{F}}{\partial \mathbf{U}} = \begin{pmatrix} 0 & 0 & 1 \\ -uv & v & u \\ -v^2 + gh & 0 & 2v \end{pmatrix}.$$

As mentioned earlier, it will be useful later on in the paper to express the equations in terms of the primitive variables

$$\mathbf{V} = (h , u , v)^T \tag{3.4}$$

in a non-conservative way, as follows,

$$\frac{\partial \mathbf{V}}{\partial t} + G \frac{\partial \mathbf{V}}{\partial x} + H \frac{\partial \mathbf{V}}{\partial y} = 0, \tag{3.5}$$

where the new matrices G and H are,

$$G = \left(\begin{array}{ccc} u & h & 0 \\ g & u & 0 \\ 0 & 0 & u \end{array}\right) \ , \ H = \left(\begin{array}{ccc} v & 0 & h \\ 0 & v & 0 \\ g & 0 & v \end{array}\right).$$

It is worth noting that the transformation matrix, M, has the form

$$M = \frac{\partial \mathbf{U}}{\partial \mathbf{V}} = \begin{pmatrix} 1 & 0 & 0 \\ u & h & 0 \\ v & 0 & h \end{pmatrix}.$$

In the conservative formulation, the fluctuation is defined as

$$\Phi_T = \int_T \mathbf{U}_t dS = -\int_T (\mathbf{E}_x + \mathbf{F}_y) dS.$$
 (3.6)

We can use the relation between the two sets of variables to define new matrices R and S,

$$R = \frac{\partial \mathbf{E}}{\partial \mathbf{V}} = \frac{\partial \mathbf{E}}{\partial \mathbf{U}} \frac{\partial \mathbf{U}}{\partial \mathbf{V}} = AM$$
$$S = \frac{\partial \mathbf{F}}{\partial \mathbf{V}} = \frac{\partial \mathbf{F}}{\partial \mathbf{U}} \frac{\partial \mathbf{U}}{\partial \mathbf{V}} = BM$$

so that:

$$\mathbf{E}_x + \mathbf{F}_y = \mathbf{E}_V \mathbf{V}_x + \mathbf{F}_V \mathbf{V}_y = R \mathbf{V}_x + S \mathbf{V}_y.$$

Provided that the variables V are linear over the cells T, the gradients,  $V_x$  and  $V_y$ , are constant, and this enables us to write the fluctuation as

$$\Phi_{T} = -\left(\int_{T} (R(\mathbf{V})\mathbf{V}_{x} + S(\mathbf{V})\mathbf{V}_{y})dS \right)$$

$$= -\left(\int_{T} (R(\mathbf{V})dS)\mathbf{V}_{x} - \left(\int_{T} (S(\mathbf{V})dS)\mathbf{V}_{y}\right)\right)$$

$$= -S_{T}[\bar{R}\mathbf{V}_{x} + \bar{S}\mathbf{V}_{y}] \tag{3.7}$$

with the definitions:

$$\bar{R} = \frac{1}{S_T} \int_T R(\mathbf{V}) dS , \ \bar{S} = \frac{1}{S_T} \int_T S(\mathbf{V}) dS.$$
 (3.8)

We now replace  $\bar{R}$ ,  $\bar{S}$  by

$$\bar{R} = R(\bar{\mathbf{V}}) , \ \bar{S} = S(\bar{\mathbf{V}})$$
 (3.9)

where the averaged variables are simply

$$\bar{\mathbf{V}} = \begin{pmatrix} \bar{h} \\ \bar{u} \\ \bar{v} \end{pmatrix} = \frac{1}{3} \begin{pmatrix} h_1 + h_2 + h_3 \\ u_1 + u_2 + u_3 \\ v_1 + v_2 + v_3 \end{pmatrix}$$
(3.10)

summing over the nodal values at the vertices of the triangle T. Note that with this definition of  $\bar{R}$ ,  $\bar{S}$  we are only approximating equation (3.8), unlike in the uler equations where an exact representation of the integral is obtained because in this case R is linear in  $\mathbf{V}$ .

We are seeking a conservative discrete approximation of the Jacobians satisfying

$$(\Phi_T \approx) - S_T(\bar{\mathbf{E}}_x + \bar{\mathbf{F}}_y) = -S_T(\bar{A}\bar{\mathbf{U}}_x + \bar{B}\bar{\mathbf{U}}_y). \tag{3.11}$$

From (3.7) it is easy to identify

$$\begin{aligned}
\bar{\mathbf{E}}_x &= \bar{R}\mathbf{V}_x \\
\bar{\mathbf{F}}_y &= \bar{S}\mathbf{V}_y.
\end{aligned} (3.12)$$

Moreover, we can use the change of variables to define

$$S_T \bar{\mathbf{U}}_x = \int_T \mathbf{U}_x dS = \int_T M(\mathbf{V}) \mathbf{V}_x dS = S_T M(\bar{\mathbf{V}}) \mathbf{V}_x$$

so that

with similar expressions for  $\bar{y}$  and y. This can be used to rewrite the fluctuation in terms of suitable averages of the conserved variables,

T

x y

\_\_\_\_

 $\theta$   $\theta$ 

 $\theta$ 

heta

and

$$=\frac{d}{d\xi} \quad _{\theta},$$

it follows from (4.1) that

$$\lambda_{\theta} \frac{d}{d\xi} + ( - + - ) \longrightarrow 0$$

which means that  $\frac{d\mathbf{V}}{d\xi}$  are the right eigenvectors of the matrix

$$^* = ^- + ^- \tag{4.2}$$

and  $\theta$  the corresponding eigenvalues.

It is then possible to express the gradient as the sum

$$= \sum_{k=1}^{n} k k k$$
 (4 3)

that is,

$$x = \begin{bmatrix} n & k & k & k \\ k=1 & & & k \\ & & k=1 & & k \end{bmatrix}$$

The vectors k are the right eigenvectors of the matrix \*:

The variables  $\ ^k$  represent weighting coefficients of the sum and  $\ ^k$  are the different angles of each wave. The celerity, , is the equivalent of the speed of sound in gas-dynamics and is the velocity of small perturbations in still water, given by = .

The connection expressed in (3.13) between the gradient of the primitive variables and that of the averaged conservative variables can be used to develop the latter as

where now, c represent the right eigenvectors of the matrix

$$_{c}^{*} = - + -$$

and can be worked out through  $\frac{k}{c} = (\ \ )^k$ . It is worth noting here that the two matrices  $\ \ ^*$  and  $\ \ ^*$  share the unique set of eigenvalues,  $\ \ ^k$ ,

The residual then can be split into a sum of waves

$$n \\ k \quad k \quad k$$

$$k=1$$

1 2 3 — 4 —

be defined in terms of the solution as

$$\phi = \theta - \frac{\pi}{4} sign(\beta).$$

Making use of the equivalences of the basic trigonometric functions to those of the first quadrant of the unit radius circle, the system (4.7) can be explicitly written as follows:

$$\frac{\partial h}{\partial x} = \alpha_1 \cos\theta - \alpha_2 \cos\theta - \alpha_3 \sin\theta + \alpha_4 \sin\theta 
\frac{\partial h}{\partial y} = \alpha_1 \sin\theta - \alpha_2 \sin\theta + \alpha_3 \cos\theta - \alpha_4 \cos\theta 
\frac{\partial u}{\partial x} = \frac{g}{c} [\alpha_1 \cos^2\theta + \alpha_2 \cos^2\theta + \alpha_3 \sin^2\theta + \alpha_4 \sin^2\theta] - \beta \sin\phi \cos\phi 
\frac{\partial u}{\partial y} = \frac{g}{c} [\alpha_1 \sin\theta \cos\theta + \alpha_2 \sin\theta \cos\theta - \alpha_3 \sin\theta \cos\theta - \alpha_4 \sin\theta \cos\theta] - \beta \sin^2\phi 
\frac{\partial v}{\partial x} = \frac{g}{c} [\alpha_1 \sin\theta \cos\theta + \alpha_2 \sin\theta \cos\theta - \alpha_3 \sin\theta \cos\theta - \alpha_4 \sin\theta \cos\theta] + \beta \cos^2\phi 
\frac{\partial v}{\partial y} = \frac{g}{c} [\alpha_1 \sin^2\theta + \alpha_2 \sin^2\theta + \alpha_3 \cos^2\theta + \alpha_4 \cos^2\theta] + \beta \sin\phi \cos\phi.$$
(4.8)

The solution of the above algebraic system is easily found giving, for the coefficient of the shear wave,

$$\beta = |\beta| \operatorname{sign}(\beta) = v_x - u_y. \tag{4.9}$$

The identities

$$\beta(\cos^2\phi - \sin^2\phi) = |\beta| \sin 2\theta$$
$$2\beta \sin\phi \cos\phi = -|\beta| \cos 2\theta$$

are helpful in combining the derivatives as

$$u_y + v_x = \left[\frac{g}{c}(\alpha_1 + \alpha_2 - \alpha_3 - \alpha_4) + |\beta|\right] \sin 2\theta$$
$$u_x - v_y = \left[\frac{g}{c}(\alpha_1 + \alpha_2 - \alpha_3 - \alpha_4) + |\beta|\right] \cos 2\theta$$

so that

$$tan2\theta = \frac{u_y + v_x}{u_x - v_y}. (4.10)$$

Further manipulations of the derivatives lead us to

$$u_x \cos^2 \theta - v_y \sin^2 \theta = \left[\frac{g}{c}(\alpha_1 + \alpha_2) + \frac{1}{2}|\beta|\right] \cos 2\theta$$

 $\quad \text{and} \quad$ 

$$h_x cos\theta + h_y sin\theta = \alpha_1 - \alpha_2,$$

hence, to the values

$$\alpha_1 = \frac{1}{2} \left[ h_x \cos\theta + h_y \sin\theta + \frac{c}{g} \left( \frac{u_x \cos^2\theta - v_y \sin^2\theta}{\cos 2\theta} - \frac{1}{2} |\beta| \right) \right]$$
(4.11)

$$\alpha_2 = \frac{1}{2} \left[ -(h_x cos\theta + h_y sin\theta) + \frac{c}{g} \left( \frac{u_x cos^2\theta - v_y sin^2\theta}{cos2\theta} - \frac{1}{2} |\beta| \right) \right].$$
 (4.12)

A similar procedure gives

$$\alpha_3 = \frac{1}{2} \left[ h_y \cos\theta - h_x \sin\theta + \frac{c}{q} \left( \frac{v_y \cos^2\theta - u_x \sin^2\theta}{\cos^2\theta} + \frac{1}{2} |\beta| \right) \right]$$
(4.13)

$$\alpha_4 = \frac{1}{2} \left[ -(h_y cos\theta - h_x sin\theta) + \frac{c}{g} \left( \frac{v_y cos^2\theta - u_x sin^2\theta}{cos2\theta} + \frac{1}{2} |\beta| \right) \right]. \quad (4.14)$$

### 4.2 Rudgyard's wave models

These are mainly based on the idea of obtaining the six waves by choosing two, in principle, arbitrary propagation angles,  $\theta_1$  and  $\theta_2$ , and performing a decomposition of the gradient,

$$\nabla \mathbf{V} = \sum_{k=1}^{3} \alpha_{\theta 1}^{k} \mathbf{r}_{\theta 1}^{k} \mathbf{n}_{\theta 1} + \sum_{k=1}^{3} \alpha_{\theta 2}^{k} \mathbf{r}_{\theta 2}^{k} \mathbf{n}_{\theta 2}$$
(4.15)

which contains six free parameters, the six  $\alpha$  coefficients. The vectors  $\mathbf{n}_{\theta} = (\cos\theta, \sin\theta)$  are again the unit vectors in the directions  $\theta$ , and  $\mathbf{r}_{\theta}^k$  are the right eigenvectors of the matrix  $M^*$  for each value of  $\theta$ . In order to solve for the unknowns, use is also made of the left eigenvectors of that matrix

$$\mathbf{l}_{\theta}^{1} = \begin{pmatrix} \frac{1}{2} \\ \frac{c}{2g} cos\theta \\ \frac{c}{2g} sin\theta \end{pmatrix}, \ \mathbf{l}_{\theta}^{2} = \begin{pmatrix} \frac{1}{2} \\ -\frac{c}{2g} cos\theta \\ -\frac{c}{2g} sin\theta \end{pmatrix}, \ \mathbf{l}_{\theta}^{3} = \begin{pmatrix} 0 \\ -sin\theta \\ cos\theta \end{pmatrix}$$
(4.16)

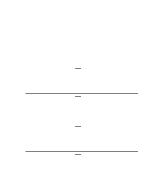
and of the unit vector normal to  $\mathbf{n}_{\theta}$ 

$$\mathbf{s}_{\theta} = (-\sin\theta, \cos\theta).$$

Multiplication of (4.16) on the left by  $\mathbf{l}_{\theta 1}^1$  and the left projection over  $\mathbf{s}_{\theta 2}$  gives

$$\mathbf{s}_{\theta 2}.(\mathbf{l}_{\theta 1}^{1}.\nabla\mathbf{V}) = \alpha_{\theta 1}^{1}(\mathbf{s}_{\theta 2}.\mathbf{n}_{\theta 1}), \tag{4.17}$$

where the property  $\mathbf{l}_{\theta}^{i} \cdot \mathbf{r}_{\theta}^{j} = \delta_{ij}$  and the orthogonality between vectors **s** and **n** 



with  $M^2 = \frac{u^2 + v^2}{c^2}$  representing the Froude number in this case. This technique gives very good results in gasdynamics problems for supersonic flows but is not directly applicable to the subsonic case. It can nevertheless be adapted for subsonic (subcritical in our case) flows by replacing  $M^2 - 1$  with  $\max(|M^2 - 1|, \epsilon)$ , the tolerance  $\epsilon$  taking a typical value of 0.1.

#### 5 Numerical Results

The treatment of the solution at the points on the boundaries of the domain has been kept as close as possible to the theory of characteristics in 2D. In all cases, the number of physical conditions to be imposed has been determined by this theory. This number is defined [6] by the signs of the eigenvalues  $\lambda$  of the matrix

$$K = An_x + Bn_y (5.1)$$

where the boundary normal vector  $\mathbf{n}$  is the unit vector pointing into the domain. The eigenvalues are associated with the celerities of the waves. Hence, when  $\lambda$  is positive, the information travels along the normal, into the domain. When it is negative, the information goes against the normal, that is out of the domain. The subcritical cases are the most illustrative, having, at a subcritical inlet for instance,  $\mathbf{u} \cdot \mathbf{n} > 0$  and  $\mathbf{u} \cdot \mathbf{n} < c$ , so that,

$$\lambda_1 = \mathbf{u} \cdot \mathbf{n} < 0$$

$$\lambda_2 = \mathbf{u} \cdot \mathbf{n} + c > 0$$

$$\lambda_3 = \mathbf{u} \cdot \mathbf{n} - c < 0.$$

This means that there are two waves from outside and therefore, two boundary conditions have to be imposed. The wave from inside produces a numerical boundary condition. In an analogous manner, the case of a subcritical outlet requires only one imposed external boundary condition. The information that travels from inside the domain is determined by the compatibility relations which can be written for arbitrary propagation directions from the 2D theory of characteristics. These have been simplified by assuming that the derivatives along the direction tangential to the boundary are negligible. In the case of a material wall boundary, a zero normal velocity is imposed and the depth as well as tangential velocity are calculated from the compatibility conditions.

For the interior points we used the non-linear PSI advection algorithm [10] for all the test cases following but obtained very similar results with the other advection schemes. As for the wave model, the calculations correspond to Rudgyard's decomposition having been found more robust, in general, than the one corresponding to Roe's model D.

With numerical schemes it is highly desirable to be able to check their predictions against suitable test problems, preferably ones for which an exact solution is available. Such is the case for the example below, computed by a finite volume method by Alcrudo and Garcia-Navarro [1], in which an oblique hydraulic jump

0

2 2 2

 $2 \qquad \qquad 2$ 

and unlike in the case of the uler equations, most practical problems involving the shallow water equations are time-dependent, so this problem also tests the temporal accuracy of the method. The treatment of the source terms was done simply by calculation of the functions at the vertices of every cell, including these values in the updating at every time level, that is, in a pointwise manner.

The channel is 21m long and 1.4m wide at it widest part. It has a uniform bottom slope  $_{0x}$  along the direction of the main flow. The roughness of the surface (smooth steel-glass) is represented by a Manning's coefficient =0.012. Measured data of the water levels as a function of time were available at five positions along the centreline of the flume. The points of measurement are shown in Fig. 5

A dam is placed in the constriction, at = 8.5m from the origin, where the width is 0.6m. The discontinuous initial conditions consist of a horizontal surface level on the upstream side, with a depth of 0.3m just behind the dam, and a uniform water depth downstream. All velocities are initially set

2

followed that of the researchers solving the uler equations (with both the advection schemes and wave models) showing the same properties as for that system of equations.

Although the procedure is more complicated and costly than present day generalizations of 1D upwinding techniques it is based on a triangular discretization and, by taking advantage of the triangles, the disadvantages can be overcome making the schemes very competitive, and the future for them then

2

- [9] Garcia-Navarro, P. and Alcrudo, F., "A TVD scheme in finite volumes for the simulation of 2D discontinuous flows" Proceedings of the XXV IAHR Congress, Tokyo 1993.
- [10] Hubbard, M. ., "A Survey of enuinely Multidimensional Upwinding Techniques." Numerical Analysis Report, 7/93, Department of Mathematics, University of Reading, UK. 1993.
- [11] Roe, P.L., "Discrete Models for the Numerical Analysis of Time-Dependent Multidimensional as Dynamics." Journal of Computational Physics, 63, pp. 458-476, 1986.
- [12] Roe, P.L., "A Basis for Upwind Differencing of the Two-Dimensional Unsteady Euler Equations." Numerical Methods for Fluid Dynamics II, K.W.Morton and M.J.Baines editors, pp. 55-80, Oxford University Press, 1986.
- [13] Roe, P.L., Struijs, R. and Deconinck, H., "A Conservative Linearisation of the Multidimensional Euler Equations." Journal of Computational Physics, to appear.
- [14] Rudgyard, M., "Multidimensional Wave Decompositions for the Euler Equations." VKI Lecture Series, 'Computational Fluid Dynamics', 1993.
- [15] Struijs, R., Roe, P.L. and Deconinck, H., "Fluctuation Splitting Schemes for the 2D Euler Equations." VKI Lecture Series 1991-01, 'Computational Fluid Dynamics', 1991.

# List of Figures

1	Map of level lines from the numerical result obtained in the 2400	0.1
	elements grid	21
2	96 elements initial grid used for the oblique jump test case	21
3	Above: 96 elements distorted grid used for the oblique jump test	
	case	22
4	Map of level lines from the numerical result obtained in the 96	
	elements distorted grid	22
5	Unsteady flow through a converging diverging channel. Geometry	
	and points of measurement	23
6	Test case $S_{0x} = 0.0$ , $h_1 = 0.3$ m, $h_2 = 0.053$ m. Continuous line: Pre-	
	dicted values. Circles: Measured values. Section 2	24
7	Test case $S_{0x} = 0.0$ , $h_1 = 0.3$ m, $h_2 = 0.053$ m. Continuous line: Pre-	
	dicted values. Circles: Measured values. Section 3	24
8	Test case $S_{0x} = 0.0$ , $h_1 = 0.3$ m, $h_2 = 0.053$ m. Continuous line: Pre-	
	dicted values. Circles: Measured values. Section 5	25
9	Test case $S_{0x} = 0.0$ , $h_1 = 0.3$ m, $h_2 = 0.053$ m. Continuous line: Pre-	
	dicted values. Circles: Measured values. Section 6	25
10	Test case $S_{0x} = 0.01$ , $h_1 = 0.3$ m, $h_2 = 0.0$ m. Continuous line: Pre-	
	dicted values. Circles: Measured values. Section 2	26
11	Test case $S_{0x} = 0.01$ , $h_1 = 0.3$ m, $h_2 = 0.0$ m. Continuous line: Pre-	
	dicted values. Circles: Measured values. Section 3	26
12	Test case $S_{0x} = 0.01$ , $h_1 = 0.3$ m, $h_2 = 0.0$ m. Continuous line: Pre-	
	dicted values. Circles: Measured values. Section 5	27
13	Test case $S_{0x} = 0.01$ , $h_1 = 0.3$ m, $h_2 = 0.0$ m. Continuous line: Pre-	
	dicted values. Circles: Measured values. Section 6	27

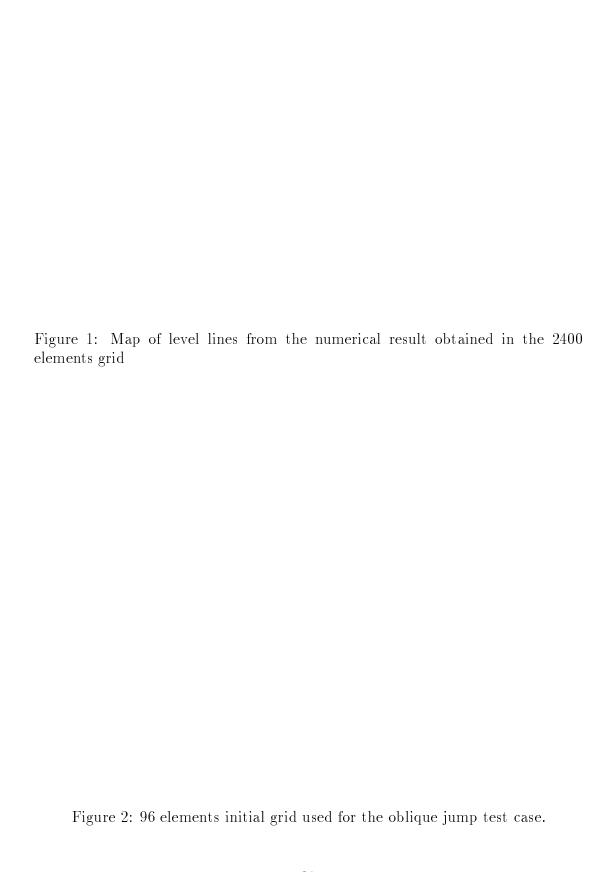


Figure 5: Unsteady flow through a converging diverging channel. Geometry and points of measurement

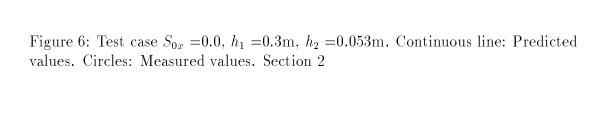


Figure 7: Test case  $S_{0x}=0.0,\ h_1=0.3\mathrm{m},\ h_2=0.053\mathrm{m}.$  Continuous line: Predicted values. Circles: Measured values. Section 3

Figure 10: Test case  $S_{0x}=0.01,\ h_1=0.3\mathrm{m},\ h_2=0.0\mathrm{m}.$  Continuous line: Predicted values. Circles: Measured values. Section 2

Figure 11: Test case  $S_{0x}=0.01,\ h_1=0.3\mathrm{m},\ h_2=0.0\mathrm{m}.$  Continuous line: Predicted values. Circles: Measured values. Section 3

Figure 12: Test case  $S_{0x}=0.01$ ,  $h_1=0.3$ m,  $h_2=0.0$ m. Continuous line: Predicted values. Circles: Measured values. Section 5

Figure 13: Test case  $S_{0x}=0.01,\ h_1=0.3\mathrm{m},\ h_2=0.0\mathrm{m}.$  Continuous line: Predicted values. Circles: Measured values. Section 6